Electronic interaction of individual slow highly charged ions with TiO_2(110)

Masahide Tona,[1,2,*] Yuso Fujita,[1] Chikashi Yamada,[1] and Shunsuke Ohtani[1,2]
[1]*Institute for Laser Science and Department of Applied Physics and Chemistry, University of Electro-Communications, Chofu, Tokyo 182-8585, Japan*
[2]*CREST, Japan Science and Technology Agency, Chofu, Tokyo 182-8585, Japan*
(Received 19 February 2008; published 18 April 2008)

A TiO_2(110) surface was bombarded with slow iodine highly charged ions (HCIs), I^{q+}, having a wide range of charge states from Ni-like I^{25+} to He-like I^{51+}. A scanning tunneling microscopic observation revealed that nanometer-sized hillock or crater structures were created by individual HCI impacts and the size of the structures increased with q. In time-of-flight secondary-ion mass spectrometry, a strong q dependence of the secondary-ion yield of O^+, $Y(O^+)$ was observed; $Y(O^+)$ exceeded $Y(Ti^+)$ for $q \sim 35$. We discuss that these secondary effects are the results of the strong coupling of HCIs with electrons in the valence band of the target.

DOI: 10.1103/PhysRevB.77.155427 PACS number(s): 79.20.Rf, 68.43.Mn, 68.47.Gh, 68.49.Sf

A slow highly charged ion (HCI) is one of the most active particles reacting violently with matter, e.g., an electron, atom, molecule, cluster and solid surface.[1–3] Here, the term "slow" means that the velocity of the ion is lower than the Bohr velocity. An interaction of a slow HCI with a surface starts with the multiple electron transfer from the surface to the approaching HCI. The slow incident ion may have sufficient time for capturing many electrons before the ion arrives at the surface. The electronic system of the surface is, in turn, excited through this process. Consequently, it is believed that effects such as secondary ion and neutral emission, the excitation of plasmons and excitons, and the dislocation of surface atoms are induced. Since the charge transfer cross section increases rapidly with incident ion charge q, these effects would be enhanced in a higher-q HCI impact. The mechanism of these phenomena is considered to be essentially different from that induced by energetic neutrals and singly charged ions where only the kinetic energy of the primary particle plays a major role.

It is considered that the secondary effects are induced in close relation with the electronic property of a target material. The active electron density is thought to be one of the most important parameters for governing the degree of the effects. In a recent report of a careful observation of dislocations on a gold surface (metal target) bombarded with Xe^{q+} ($q \leqq 44$),[4] it was shown that nanometer sized structures were created by the nuclear stopping power of the primary ions rather than by the multiple electron transfer; that is, no q dependence was observed. Meanwhile, in our previous work,[5] it was revealed that the secondary effects were enhanced with q on a Si(111)-(7×7) surface (semiconductor target) by individual HCI impacts (I^{q+}, $q \geqq 30$).

Oxide material is important as the target in the HCI-surface interaction study. Because it is a compound insulator, we may clarify the effect of the electronic property on the HCI impact in contrast to elemental metals or semiconductors, e.g., by directly observing the HCI-irradiated surface. Further interest lies upon HCI-based nanoprocessing, e.g., the fabrication to thin film oxides of tunnel junctions for superconducting devices.[6] In this paper, we show remarkable features of the interaction of high-q HCIs with an oxide target. A TiO_2(110) surface was employed because a clean well-defined surface is easy to obtain and is observable with atomic resolution using a scanning tunneling microscope (STM).[7] A typical nanostructure induced by a single I^{51+} impact has a "calderalike" shape, as shown in a STM image in Fig. 1. We present the morphological change in such impact sites with various q-HCI impacts, together with the q dependence of the secondary-ion yield, measured with time-of-flight secondary-ion mass spectrometry (TOF-SIMS). We discuss the mechanism in the HCI-oxide-surface interaction, based on the so-called Coulomb explosion model in which the explosion is thought to be caused by the "desorption induced by electronic transition (DIET)" process. The characteristics of the HCI-DIET are revealed by comparison with the Knotek–Feibelman (KF) mechanism[8] as another DIET process.

In the course of the investigation, we have developed an *in situ* observation system installed in the Tokyo-EBIT (electron beam ion trap) facility.[9–11] I^{q+}-HCIs were used with a wide range of q from Ni-like I^{25+} to He-like I^{51+}. Details of the methods for the observations under the ultrahigh vacuum condition (base pressure: 2×10^{-8} Pa) were described

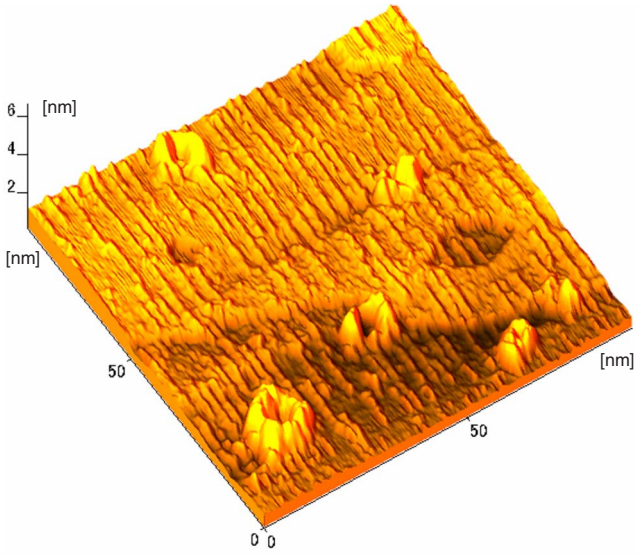

FIG. 1. (Color online) STM image of impact sites on a TiO_2(110) surface created by individual I^{51}-HCI bombardments.

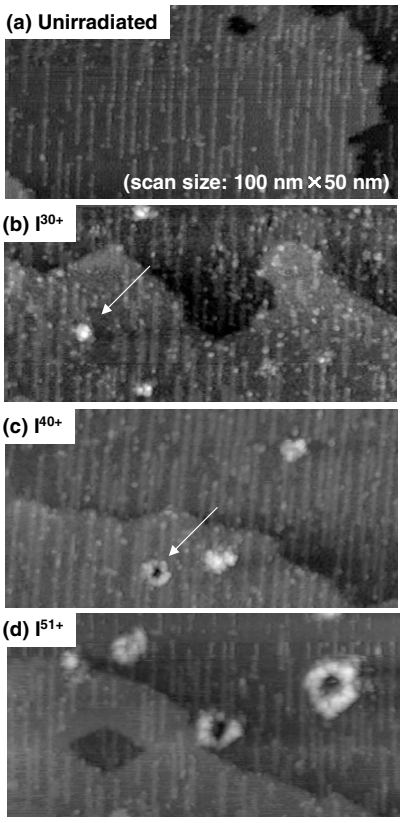

FIG. 2. STM images of a TiO_2(110) surface; (a) unbombarded area, (b) I^{30+}, (c) I^{40+}, and (d) I^{51+} impacts. The kinetic energies of the incident ions were identically 150 keV.

elsewhere.[5,12] A well-defined TiO_2(110) surface was prepared by an ordinary method of repetition of annealing and ion-sputtering procedures, as reported in Ref. 7. The data acquisition time for obtaining a TOF spectrum was approximately the same for all charge states and less than 15 min in all cases. The sample was irradiated by HCIs for several hours, transferred to the observation chamber without breaking the vacuum, and then observed with STM. This procedure was carried out as a consecutive motion.

Figure 2(a) shows a typical STM image of the TiO_2 (110) surface before HCI bombardments. The scan size is 100×50 nm^2. The image was obtained with the sample bias of +2 V. Line defects of Ti_2O_3 are seen as brighter rows on a large, atomically flat terrace.[7] The images (b), (c), and (d) were observed after the bombardments of I^{q+}-HCIs with $q=30$, 40, and 51, respectively. The scan size and the observation condition are the same as those for image (a). The kinetic energies, E_K (=150 keV) of incident I^{q+} ($q=30$, 40, and 51) were identical in order to discriminate q dependence in the effect of the HCI-surface interaction. Nanometer sized structures can be found in addition to the line defects. The density of these sites was nearly equal to the HCI dose.[13] In (b), with I^{30+} impacts, hillocklike impact sites are observed, as indicated by a white arrow. For the I^{40+} impact (c), it can be seen that a larger hillock structure was created. In addition, a crater structure was observed, as indicated by an arrow. The size of these structures increases with q as shown in (d) for I^{51+} impacts.

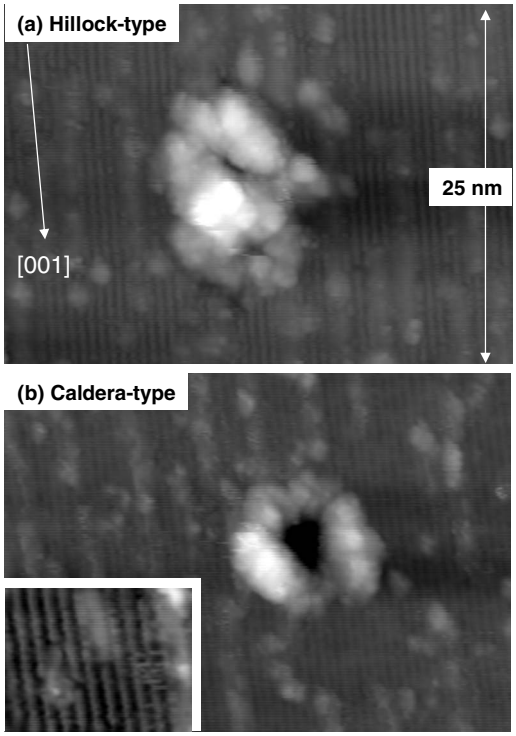

FIG. 3. Close-up images of I^{51+}-impact sites on a TiO_2(110) surface. Two kinds of structures, (a) hillocklike and (b) calderalike were observed. The inset of (b) shows the atomic image of the TiO_2(110) surface. The spacing of the stripes is ~0.6 nm.

Figure 3 shows (a) hillocklike and (b) craterlike impact sites, induced by single I^{51+} bombardments. The heights of these structures are much higher than that of an atomic step (~0.3 nm) (see also Fig. 1). The inset of (b) shows a close-up image of an unbombarded portion in which the atomic structure of TiO_2(110) can be seen; dark and bright stripes are parallel to the [001] direction corresponding to oxygen and titanium rows, respectively, and the spacing of the stripes is about 0.6 nm.[7] It is found by the present observation with atomic resolution that the surface of the hillock is not smooth but rough with irregularities. Such a fine structure could not be observed in the images for insulator surfaces, e.g., CaF_2, as previously reported,[14,15] using an atomic force microscope having lower resolution than the STM. The height and diameter of the hillock are measured to be ~1 nm and ~10 nm, respectively. On the other hand, the crater structure has an outer rim whose height is also ~1 nm. The depth of the crater is measured to be at least 1.5 nm, although it depends on the shape of the tip used. The size of the crater (both height and depth) is much larger than that created on a Si(111)-(7×7) surface.[5]

A dramatic HCI-impact effect on the oxide target is also observed in the secondary-ion emission. Figure 4(a) shows a typical TOF-SIMS spectrum obtained from a TiO_2 (110) surface bombarded with I^{50+}-HCIs having $E_K=175$ keV. O^+ is seen as the most intense peak together with small contributions from other fragment ions, as represented in the figure. The peaks associated with calcium originate in an impurity commonly present in commercially available TiO_2 crystal; it is known that Ca segregates to the surface during the anneal-

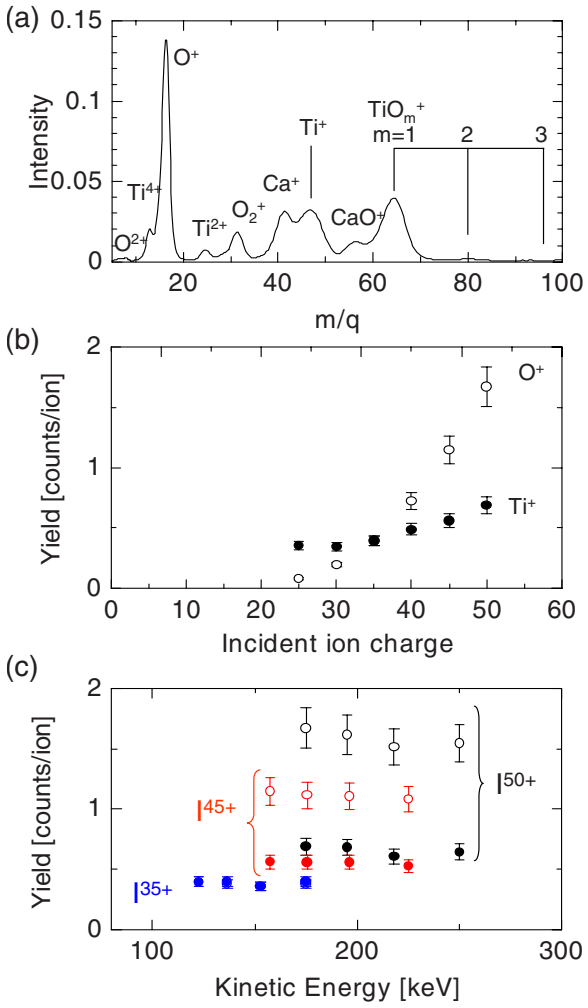

FIG. 4. (Color online) (a) TOF-SIMS spectrum from a TiO_2 (110) surface bombarded with I^{50+}-HCIs. (b) Secondary-ion yields for O^+ (open circles) and Ti^+ (solid circles) as a function of incident ion charge q. Kinetic energy of the incident projectile was $q \times 3.5$ keV. (c) Secondary-ion yields for O^+ (open circles) and Ti^+ (solid circles) as a function of the kinetic energy of the primary projectiles.

ing procedure.[16] Figure 4(b) shows the secondary-ion yields for O^+, $Y(O^+)$ (open circles) and for Ti^+, $Y(Ti^+)$ (solid circles) as a function of q. The error was estimated to be 10%, coming mainly from the collection efficiency for the sputtered ions in the TOF-SIMS measurements. For the low-q HCI impacts ($q=25$), $Y(O^+)$ is much smaller than $Y(Ti^+)$. With increasing q, $Y(O^+)$ increases much more rapidly than $Y(Ti^+)$ and the peak of O^+ grows to be the most intense in the TOF spectrum, as shown in Fig. 4(a). Although E_K of the incident projectile in Fig. 4(b) was $q \times 3.5$ keV, varying from 87.5 ($q=25$) to 175 keV ($q=50$), it seems that the increase in E_K does not significantly affect the q dependence of the yields in this range. Figure 4(c) shows the E_K dependences of $Y(O^+)$ (open circles) and $Y(Ti^+)$ (solid circles), obtained with I^{q+} impacts ($q=35$, 45, and 50). Note that since $Y(O^+)$ is nearly equal to $Y(Ti^+)$ for $q=35$, the plotted circles overlap each other. It can be seen from the result that the secondary-ion yields are not dependent on E_K but on q in this energy region.

It is a striking feature of the secondary-ion emission from the oxide target bombarded with high-q HCIs that O^+ is detected most frequently, and furthermore, O^{2+} ions are clearly observed [see Fig. 4(a)]. A similar result has also been obtained in the measurement with a SiO_2 thin film on a Si substrate (SiO_2/Si), as previously reported.[17] This behavior is difficult to observe with irradiation of a singly charged ion, except under a special condition for the coupling of a target with a primary projectile such as the interatomic transition of a core level electron of TiO_2 to He^+.[18] It is well known in the secondary-ion emission induced by the kinetic effect that oxygen ions are detected as negative ions rather than positive ions. This is due to the nature of the oxygen atom that has both high electron affinity and high ionization potential. In our measurement, $Y(O^+)$ is so small that very weak signals are measured in the TOF spectrum for low-q HCI impacts.

The high emission yield of the positively charged oxygen ions with a high-q HCI impact might be explained by the multiple electron transfer in the interaction of the HCI with the surface. As is clear from the measurement for the yield of secondary electron emission,[19] such a high-q HCI, e.g., $q=50$, captures more than a hundred electrons from the target during the interaction. According to the "classical over-the-barrier model",[20] in the collision of a HCI with an insulator surface, many electrons in the valence band are transferred to high Rydberg states of the HCI. The valence band of TiO_2 is mainly composed of oxygen $2p$ states although it is somewhat covalent (the fraction of ionic character is ~60%). This means that electrons captured by the HCI should be fed mainly from oxygen atoms near the surface. When negatively charged oxygen in TiO_2 before the interaction is neutralized by the electron transfer, the portion of the binding energy due to ionic character will be released. Furthermore, varying of the oxygen from neutral to a positive ion by the second electron transfer induces instability of the surface structure due to Coulomb repulsion. As a result, secondary particles, i.e., fragment ions shown in the TOF spectrum and/or possibly neutrals, will be emitted by the Coulomb explosion.[21]

The process may be considered as a special kind of DIET; the Coulomb explosionlike sputtering is induced by the multiple electron transfer, resulting in the large $Y(O^+)$ by the high-q HCI impact. The KF mechanism is well known for explaining the O^+ emission induced by DIET.[8] The KF mechanism is that O^+ in an oxide material is generated by the interatomic and intra-atomic Auger processes which are triggered by the creation of a core hole with the energetic electron or photon impact. Unlike an indirect ionization as in the KF mechanism, O^+ is directly created by multiple electron transfer through the strong coupling of the high-q HCI with electrons in the valence band. While $Y(O^+)$ increases with the electron or photon energy in the KF mechanism, it depends strongly on q but not on E_K in the case of the HCI impact. This is due to the electron-capture cross section's being largest among those of other relevant processes, almost independent of E_K and definitely increasing with q.

The singular property of the HCI-DIET processes is that more than one secondary ion are emitted by a single high-q HCI impact, or in other words, the secondary-ion yield becomes greater than one. This high emission yield is never

achieved by a single electron or photon impact. A small enhancement of positive ion yield by "moderate" interaction with low-q HCIs was also observed.[22] It was considered that the emission was induced by defect mediated sputtering. This mechanism is well known as a kind of normal DIET and is also observed when the target such as an alkali halide crystal, which has strong electron-lattice coupling, is irradiated by electrons and photons. This is quite different from that induced by the violent interaction shown in the present work. The total secondary-ion yield, Y_{tot}, from TiO_2, evaluated by numerically integrating the areas shown in Fig. 4(a), reaches 4.4 ions per I^{50+}-HCI. A similar result has also been obtained in the measurement for SiO_2/Si (3.5 ions/I^{50+}). These total yields are much larger than that for Si (0.6 ions/I^{50+}). The high emission yield from the oxide target is consistent with the fact that individual HCI impacts are able to strongly modify the surface structures of the oxides.

Surprisingly, from the size of the crater or hillock in Fig. 3, we estimated that a few hundred up to a thousand atoms are moved or sputtered by the impact of a single I^{51+}; while only a few secondary ions are emitted. According to the previous observation of the Coulomb sputtering from UO_2 bombarded high-q HCI,[23] about 100 neutral atoms are sputtered while the secondary-ion yield is very low, which is the same as that in our case. Further, it is made clear that the same or larger number of atoms as the sputtered neutral atoms is moved from the initial lattice sites and from the large impact site. We consider that the resultant shape of the impact site depends on the strength of the Coulomb explosion in which most of the positive ions are neutralized. In a low-q HCI impact, electrostatic energy stored in the charged domain would be relatively small because the number of electrons transferred is small. For example, $Y_{\mathrm{tot.}}$ at $q=30$ barely exceeds unity, where the contribution of O^+ to $Y_{\mathrm{tot.}}$ is only ~20%, while it reaches ~40% of $Y_{\mathrm{tot.}}$ (~4) for I^{50+} impact. In such a weak interaction of a lower-q HCI, although titanium and oxygen are removed from the initial lattice sites, not all could be completely sputtered into the vacuum. As a result, some are heaped on the surface and the hillocklike structure is created. Since the surface area from which the electrons are removed becomes larger for higher q, a larger hillock impact site is seen, as shown in Fig. 2. In addition, the higher energy stored in the electron-depletion area induces the emission of a larger number of secondary particles and creates a calderalike structure by a violent explosion.

This work has been supported by the CREST program, "Creation of Ultrafast, Ultralow Power, Super-performance Nanodevices and Systems" in the Japan Science and Technology Agency, and has been performed as an activity under the 21st Century Center of Excellence (COE) Program, "Innovation in Coherent Optical Science" at the University of Electro-Communications.

*tona@ils.uec.ac.jp

[1] A. Arnau, F. Aumayr, P. M. Echenique, M. Grether, W. Heiland, J. Limburg, R. Morgenstern, P. Roncin, S. Schippers, R. Schuch, N. Stolterfoht, P. Varga, T. M. J. Zouros, and H. P. Winter, Surf. Sci. Rep. **27**, 113 (1997).
[2] T. Schenkel, A. V. Hamza, A. V. Barnes, and D. H. Schneider, Prog. Surf. Sci. **61**, 23 (1999).
[3] J. D. Gillaspy, J. Phys. B **34**, R93 (2001).
[4] J. M. Pomeroy, A. C. Perrella, H. Grube, and J. D. Gillaspy, Phys. Rev. B **75**, 241409(R) (2007).
[5] M. Tona, H. Watanabe, S. Takahashi, N. Nakamura, N. Yoshiyasu, M. Sakurai, T. Terui, S. Mashiko, C. Yamada, and S. Ohtani, Surf. Sci. **601**, 723 (2007).
[6] J. M. Pomeroy, H. Grube, A. C. Perrella, and J. D. Gillaspy, Appl. Phys. Lett. **91**, 073506 (2007).
[7] U. Diebold, Surf. Sci. Rep. **48**, 53 (2003), and references therein.
[8] M. L. Knotek and P. J. Feibelman, Phys. Rev. Lett. **40**, 964 (1978).
[9] H. Watanabe, J. Asada, F. J. Currell, T. Fukami, T. Hirayama, K. Motohashi, N. Nakamura, E. Nojikawa, S. Ohtani, K. Okazaki, M. Sakurai, H. Shimizu, N. Tada, and S. Tsurubuchi, J. Phys. Soc. Jpn. **66**, 3795 (1997).
[10] H. Shimizu, F. J. Currell, S. Ohtani, E. J. Sokell, C. Yamada, T. Hirayama, and M. Sakurai, Rev. Sci. Instrum. **71**, 681 (2000).
[11] M. Tona and S. Takahashi, J. Phys.: Conf. Ser. **2**, 57 (2004).
[12] M. Tona, K. Nagata, S. Takahashi, N. Nakamura, N. Yoshiyasu, M. Sakurai, C. Yamada, and S. Ohtani, Surf. Sci. **600**, 124 (2006).
[13] N. Yoshiyasu, S. Takahashi, M. Shibata, H. Shimizu, K. Nagata, N. Nakamura, M. Tona, M. Sakurai, C. Yamada, and S. Ohtani, Jpn. J. Appl. Phys., Part 1 **45**, 995 (2006).
[14] I. C. Gebeshuber, S. Cernusca, F. Aumayr, and H. P. Winter, Int. J. Mass. Spectrom. **229**, 27 (2003).
[15] A. S. El-Said, W. Meissl, M. C. Simon, J. R. Crespo Lòpez-Urrutia, I. C. Gebeshuber, M. Lang, H. P. Winter, J. Ullrich, and F. Aumayr, Nucl. Instrum. Methods Phys. Res. B **258**, 167 (2007).
[16] L. P. Zhang, M. Li, and U. Diebold, Surf. Sci. **412-413**, 242 (1998).
[17] M. Tona, S. Takahashi, K. Nagata, N. Yoshiyasu, C. Yamada, N. Nakamura, S. Ohtani, and M. Sakurai, Appl. Phys. Lett. **87**, 224102 (2005).
[18] R. Souda, Phys. Rev. Lett. **82**, 1570 (1999).
[19] H. Kurz, F. Aumayr, H. P. Winter, D. Schneider, M. A. Briere, and J. W. McDonald, Phys. Rev. A **49**, 4693 (1994).
[20] J. Burgdörfer, P. Lerner, and F. W. Meyer, Phys. Rev. A **44**, 5674 (1991).
[21] I. S. Bitenskii, M. N. Murakhmetov, and E. S. Parilis, Sov. Phys. Tech. Phys. **24**, 618 (1979); S. Parilis, L. M. Kishinevsky, N. Yu. Turaev, B. E. Baklitzky, F. F. Umarov, V. Kh. Verleger, S. L. Nizhnaya, and I. S. Bitensky, *Atomic Collisions on Solid Surfaces* (Elsevier Science, Amsterdam, 1993), Chap. 12.
[22] T. Neidhart, F. Pichler, F. Aumayr, H. P. Winter, M. Schmid, and P. Varga, Nucl. Instrum. Methods Phys. Res. B **98**, 465 (1995).
[23] T. Schenkel, A. V. Barnes, A. V. Hamza, D. H. Schneider, J. C. Banks, and B. L. Doyle, Phys. Rev. Lett. **80**, 4325 (1998).